The IRM Quarterly
Winter 2002-3, Vol. 12, No. 4

Inside...

Visiting Fellow Reports 2
Current Abstracts 5
New Visiting Fellows 11
RAC Rotation 11
Kudos for IRM Students 11
New Proposal Deadlines 11

Maintaining Standards II

more fun with calibration

Mike Jackson
Jim Marvin
Peat Sølheid
IRM

In a fused-quartz tube in a drawer in the high-field SQUID lab at the Institute for Rock Magnetism, a small cylinder of pure palladium is carefully stored. It is the *IRM*'s primary standard for absolute calibration of DC susceptibility, traceable to standards of the former NBS (National Bureau of Standards), now NIST (National Institute of Standards and Technology).

Palladium is perhaps a surprising material to use for a magnetic standard: of all the substances one might consider, platinum-group metals are not usually among the first that spring to mind. Yet two factors make it eminently suitable. First, it is a moderately strong paramagnet (χ_{293K}= 6.69x10^{-8} m^3/kg). Of all the elements, higher susceptibilities occur only among the lanthanides and the 4th-period transition metals. Second, it is highly resistant to oxidation in normal atmospheric conditions. Although it has been replaced by NIST with other magnetic standards, palladium was formerly supplied by NBS as standard reference material (SRM) 765, the primary standard used by Quantum Design for calibration of the MPMS superconducting susceptometer.

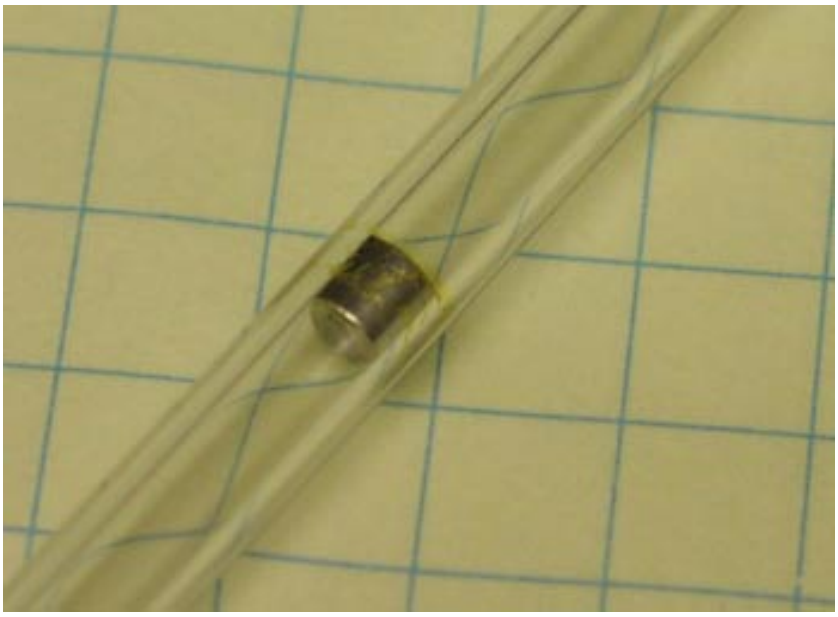

Palladium standard Pd-603, a 253-mg cylinder approximately 2 mm in diameter and 3 mm in length, is traceable to NIST standards.

NIST currently offers three magnetic SRMs, all of which are ferromagnetic: SRM762 and 772a are nickel (J_S=54.78 ± 0.15 A·m^2/kg), the former in the form of a disk and the latter as a sphere; SRM2853 is a sphere of yttrium garnet (J_S=27.6 ± 0.1 A·m^2/kg). Princeton Measurements has used both the yttrium garnets and the nickel spheres for primary calibration of their MicroMag VSMs and AGMs. Like palladium, these materials combine well-defined magnetic properties with excellent chemical stability. Moreover they are less sensitive than paramagnets are to small temperature changes. The susceptibility of a Curie-law paramagnet changes by about 0.3% per degree C of temperature change (near room T), whereas the saturation magnetization of nickel changes by only about 0.03% per degree between 10° and 30°C.

Princeton, Quantum and most other instrument manufacturers produce their own standards and distribute them with new instruments. Princeton's standards are small squares of Ni foil, less than 1 mg, sandwiched between 3-mm square glass plates. Quantum provides the aforementioned palladium cylinders (~250 mg). Kappabridges come from AGICO with ferrite standards.

Why Use Standards?

Magnetometers and susceptometers do not, as a rule, directly measure magnetization or susceptibility of a sample. What they do measure directly is a current or voltage, induced by the sample's magnetic field and its changes with time. The simplest and most direct way to translate measured voltages into a sample moment is by calibration, i.e., determining the ratio for a sample of known moment, which of course requires a

Calibration

continued on p. 7...

Mass magnetic susceptibilities [10^{-8} m^3/kg] of bulk pure metals of the transition elements at room temperature (source: CRC Handbook)

	3	4	5	6	7	8	9	10	11
4	**Sc** *44.96* 8.8	**Ti** *47.88* 4.0	**V** *50.94* 6.3	**Cr** *52* 4.3	**Mn** *54.94* 11.4	**Fe** *55.85* ferro	**Co** *58.47* ferro	**Ni** *58.69* ferro	**Cu** *63.55* -0.1
5	**Y** *88.91* 0.0	**Zr** *91.22* 1.7	**Nb** *92.91* 2.6	**Mo** *95.94* 1.2	**Tc** *98* 3.2	**Ru** *101.1* 0.5	**Rh** *102.9* 1.4	**Pd** *106.4* 6.7	**Ag** *107.9* -0.2
6	**La** *138.9* 1.1	**Hf** *178.5* 0.5	**Ta** *180.9* 1.1	**W** *183.9* 0.4	**Re** *186.2* 0.7	**Os** *190.2* 0.1	**Ir** *190.2* 0.2	**Pt** *195.1* 1.3	**Au** *197* -0.2

An Igneous Origin For Martian Magnetic Anomalies?

Julia Hammer
University of Hawaii
jhammer@soest.hawaii.edu
Stefanie Brachfeld
Ohio State University
brachfeld.2@osu.edu

Introduction: The presence of alternately magnetized sources on Mars indicates that at one time Mars had a magnetic field, presumably generated by an internal dynamo, and that its polarity reversed at least once before shutting off[1]. Mars does not currently possess a magnetic field, so the anomalies are attributed to remanent magnetization (RM) of minerals in the crust. The initiation and cessation of the inducing field, its timing, and the implications for Mars thermal evolution, compositional differentiation, and volatile budget are critical components of understanding the planetary dynamics of Mars. Isobaric (1 bar) constant-rate cooling experiments were run using Fe-rich (i.e., Martian) basalt to ascertain whether conditions necessary for crystallization of minerals retaining intense RM are consistent with any of the models proposed for generation of the Martian magnetic anomaly.

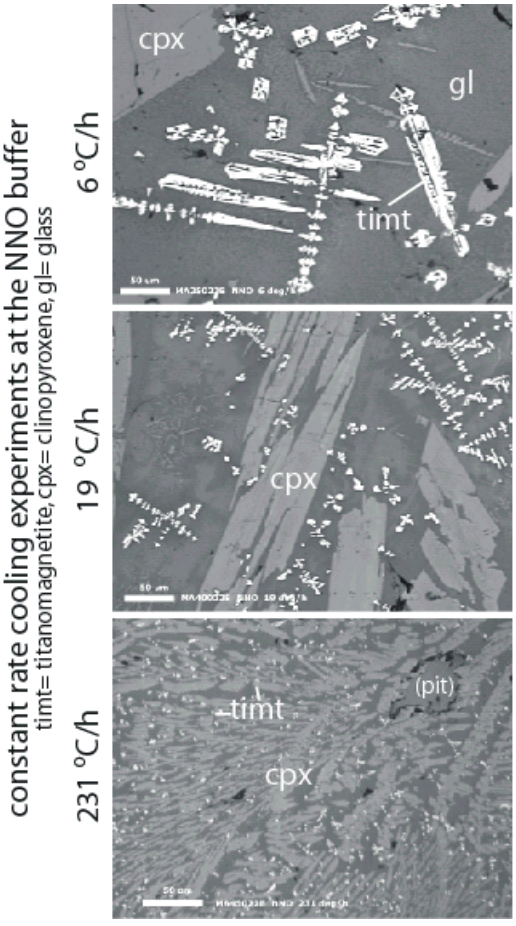

Fig. 1

Cooling experiments: The material investigated is synthetic A*, a liquid composition in equilibrium with olivine and pyroxene during crystallization of the Shergottites, Chassigny, and other cumulate SNC meteorites[2]. The compositional and rheological characteristics of A* are shared by other proposed SNC parent melts (low in Al_2O_3 and FeO-rich)[3,4].

The first series of experiments determined the near-liquidus phase relations for the A* composition over a range of fO_2 values corresponding to the Fe-wüstite (IW) to MnO-Mn_3O_4 (MNO) solid buffer assemblages. Care was taken to minimize Fe loss during the experiments: runs at the most reducing conditions were executed in Mo foil, and the intermediate to oxidizing fO_2 experiments were run in Pt capsules presaturated with Fe by running A* at the experimental temperature for 12-24 h. Sample capsules and solid buffer assemblages were loaded into fused quartz tubes, evacuated to a moderate vacuum (≤10 Pa), then sealed shut. The solid buffer assemblage was inspected at the termination of each run to confirm or bracket the experimental fO_2.

A second matrix of 24 experiments were run to examine the kinetics of low-pressure oxide crystallization as a function of fO_2 and cooling rate. Evacuated fused quartz capsules containing sample + buffer (IW, QFM, NNO, MNO) were bundled together, brought to 1210° C, then cooled to ~300° C. Five sets of constant-rate cooling experiments (230, 72, 19, 6, and 3° C h^{-1}) were run using a programmable temperature controller. Rapid (highly nonlinear, ~1.5E5° C h^{-1}) cooling was imposed by immersion of the capsules in water.

Textural characterization: A dazzling variety of titanomagnetite (TiMt) and clinopyroxene (Cpx) morphologies were produced that broadly correlate with cooling rate (Fig. 1). Texturally, there was no discernible effect of experiment *f*O2, except on the abundance of titanomagnetite in the charge. For both TiMt and Cpx, increasing experiment duration (lower cooling rate) correlates with increasing crystal content, grain size coarsening, and morphological transition from highly skeletal, cruciform (TiMt), and dendritic (Cpx) forms toward euhedral forms. Except for the MNO charge, which started below the TiMt liquidus at 1210° C, no crystallization was observed in the most rapidly cooled (10 E5° C h^{-1}) series. Long strands of collinear TiMt crystals evident in 2D images appear to represent single crystals linked outside the plane of the cut surface. These morphologies complicate the determination of crystal nucleation rate by standard image processing techniques[5] . Instead, the ratio of the mineral surface area to mineral volume is considered a measure of the surface free energy controlling nucleation kinetics in these experiments. We calculated a nondimensional index of surface energy by finding the ratio of the glass-TiMt interfacial boundary length, including internal holes, to the circumference of a single circle having the equivalent area. Preliminary measurements indicate that the index ranges over several orders of magnitude, consistently increasing in proportion to cooling rate.

Magnetic characterization: Samples from the cooling experiments were characterized for concentration of ferromagnetic material, magnetic domain state, magnetic mineralogy, ability to carry anhysteretic remanent magnetization and thermoremanent magnetization (ARM and TRM, respectively) using a suite of applied field- and temperature-dependent methods. The range of laboratory cooling rates used was sufficient to generate magnetic mineral assemblages with variable composition and magnetic domain states. Several broad trends are evident. The samples prepared at the MNO buffer have the highest saturation magnetization and the highest magnetic susceptibility for any given cooling rate. The samples prepared at the IW buffer have the lowest saturation magnetization and the lowest magnetic susceptibility for any given cooling rate. The QFM and NNO sample sets are very similar with respect to the abundance of magnetic material. Consistent with the petrographic observations, we observe a magnetic grain size coarsening with slower cooling rates for the QFM, NNO, and MNO samples. Using in-field measurements and high-temperature methods, the IW sample set appears dominantly paramagnetic with the exception of the sample synthesized at the slowest cooling rate. However, low temperature methods and induced remanences (ARM and TRM) indicate the presence of a remanence-bearing phase in the IW samples. We did not observe pure end-member magnetite or hematite. Curie temperatures range from ~300-510° C, consistent with Ti-rich titanomagnetite or Ti-rich titanohematite. Samples prepared at the MNO buffer had the highest Curie temperatures (475-495° C), with no apparent relationship to cooling rate. Samples prepared under the QFM and NNO buffers had lower Curie temperatures,

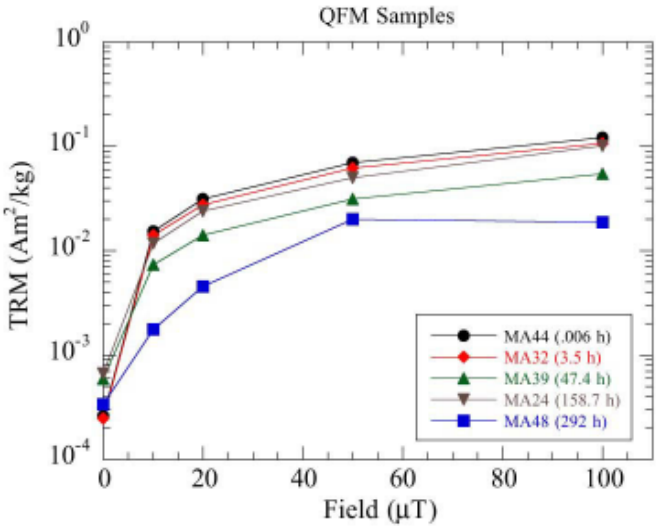

Fig. 2

although there appears to be a significant shift in mineralogy at the slowest cooling rates. Nearly all samples in the QFM, NNO, and MNO sets displayed a magnetic order/disorder transition in the 30-65K range, with no apparent relationship to cooling rate. We imparted TRM at 550° C in ambient fields of 10, 20, 50 and 100 mT (Fig. 2). At the 50 mT step, we observe TRM intensities of 0.1-70 x10^{-3} Am^2 kg^{-1} .

Summary: Magnetic characteristics of rapidly cooled A* basalt crystallized under moderate to highly oxidizing conditions are comparable to those described for rapidly cooled terrestrial basalts[6] and modeled as potential source materials for the Martian anomalies[7] .

References: [1] Stevenson D. J. (2001) *Nature 412,* 214-219. [2] Johnson M.C., Rutherford M.J., and Hess P.C. (1991) *Geochim. Cosmochim. Acta 55* 349-366. [3] McSween H.Y., Eisenhour D.D., Taylor L.A., Wadhwa M., and Crozaz G. (1996) *Geochim. Cosmochim. Acta 60* 4563-4569. [4] Wadhwa M. and Crozaz G. (1995) *Geochim. Cosmochim. Acta 59* 3629-3645. [5] Hammer, J.E. and Rutherford M.J. (2002) *J. Geophys. Res. 107* 10.1029/2001JB000281. [6] Zhou, W et al., (2000) *Earth Planet Sci Lett 179* 9-20. [7] Nimmo, F., (2000) *Geology 28* 391-394. [8] Connerney J.E.P., (1999) *Science 284* 794-798.

Low-Temperature Hysteresis and Other Magnetic Properties of Hematites

Özden Özdemir
University of Toronto
ozdemir@physics.utoronto.ca

Last year at the IRM, I investigated saturation remanence (SIRM) and temperature dependence of hysteresis of SD and MD hematites. Submicron hematites were prepared by heating SD magnetites and acicular lepidocrocites at 700° C in air for 18 hours. Commercial hematite powders were also heated in air for 5 hours at 500° C to convert any ferrimagnetic impurity to Fe_2O_3. X-ray analysis indicates that all samples have well-defined hematite diffraction patterns. No iron-containing impurities were detected.

Room-temperature hysteresis loops for the submicron hematites did not close. A 1.5 T field was not enough to saturate the magnetization, and M_{RS}/M_S and H_C values were very high. H_C ranges from 140 to 272 mT. These very high H_C's are controlled by the c-plane anisotropy, which combines uniaxial magnetoelastic and triaxial magnetocrystalline anisotropies (Özdemir and Dunlop, 2002). M_{RS}/M_S varies from 0.6 to 0.72, intermediate between expected SD values of 0.5 for magnetoelastic anisotropy and 0.75 for magnetocrystalline c-plane anisotropy. The acicular hematite has a purely uniaxial remanence ratio of 0.5.

The natural single crystal of hematites are from Quebec, Canada and Rio Marino, Italy and their grain sizes vary between 500 μm and 3 mm. Their flat surfaces are smooth, very shiny and correspond to the (0001) basal plane. The single crystals were given an SIRM along the basal plane (0001) in a field of 2.5 T at room temperature, then cooled to 20 K and back to 300 K in zero field. In cooling through the Morin transition, remanence decreased sharply with the onset of antiferromagnetism. At T_M, 96-99% of the initial SIRM had been demagnetized with the disappearance of spin-canting. The remaining 1-4% of the original remanences were temperature independent between T_M and 20 K and must be magnetoelastically pinned. This surviving defect moment is the core of the magnetic memory. The SIRM memories at room temperature were about 33-42% of the initial remanence. Similar behaviour has been observed for submicron hematites (Özdemir and Dunlop, 2002).

Hysteresis loops were measured on two millimeter-size single crystals of hematite at selected temperatures from 300 to 20 K using a low-T micro VSM. The field was applied parallel to the (0001) plane of the crystal. The shape of the hysteresis curves for both crystals showed remarkably different features below and above the Morin transition. The curves between 300 K and T_M were typical hematite hysteresis curves. The hysteresis loops at T_M were slightly constricted, indicating that the crystals consist of coexisting ferrimagnetic and antiferromagnetic phases with vastly different coercivities. Below T_M, the constriction disappeared and the loops were sheared. It is interesting to observe a hysteresis below the Morin transition since, antiferromagnetic hematite with antiparallel spin arrangement, should have no spontaneous moment. The loops are not due to magnetic impurities. The SIRM cooling and warming curves between T_M and 20 K were flat, confirming that the crystals are free of ferrimagnetic impurities. The sheared hysteresis loops below T_M could be attributed to the defect moment which plays an important role in renucleating the magnetic memory during the warming cycle.

I would like to thank Mike, Peat and Jim for their help and hospitality.

Özdemir, Ö., and D.J. Dunlop, 2002. Thermoremanence and stable memory of single-domain hematites. *Geophys. Res. Lett,* ***29***, 10.1029/2002GL015597.

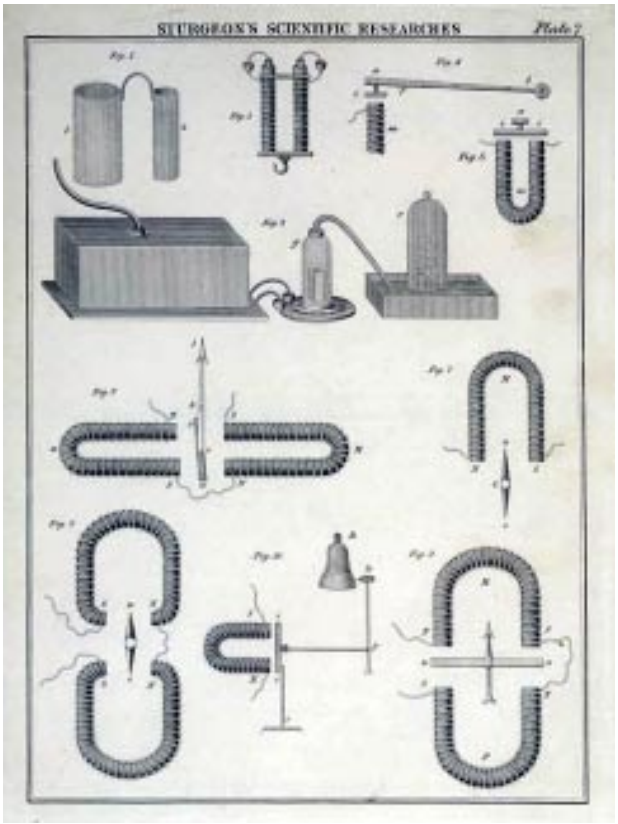

http://www.loc.gov/exhibits/british/images/vc142.jpg

Current Abstracts

A list of current research articles dealing with various topics in the physics and chemistry of magnetism is a regular feature of the IRM Quarterly. *Articles published in familiar geology and geophysics journals are included; special emphasis is given to current articles from physics, chemistry, and materials-science journals. Most abstracts are culled from* INSPEC *(© Institution of Electrical Engineers),* Geophysical Abstracts in Press *(© American Geophysical Union), and* The Earth and Planetary Express *(© Elsevier Science Publishers, B.V.), after which they are subjected to Procrustean editing and condensation for this newsletter. An extensive reference list of articles (primarily about rock magnetism, the physics and chemistry of magnetism, and some paleomagnetism) is continually updated at the* IRM. *This list, with more than 5200 references, is available free of charge. Your contributions both to the list and to the Abstracts section of the* IRM Quarterly *are always welcome.*

Anisotropy

Kelso, P. R., Tikoff, B., Jackson, M., and Sun, W., 2002, **A new method for the separation of paramagnetic and ferromagnetic susceptibility anisotropy using low field and high field methods**: *Geophysical Journal International, v. 151*, no. 2, p. 345-59.
We separate the ferromagnetic and paramagnetic components of AMS for 1-inch cylindrical samples, using a VSM for high-field (HF) directional measurements. This separation is tested by artificially combining separate samples with known paramagnetic-only and ferromagnetic-only behaviour. By comparing the HF results of a combined paramagnetic and ferromagnetic signal to the low-field k_{AC} of the paramagnetic-only signal, we demonstrate that the HF AMS is the result solely of the paramagnetic fabric even when the low field AMS is dominated by the ferromagnetic minerals.

Jezek, J., and Hrouda, F., 2002, **Software for modeling the magnetic anisotropy of strained rocks**: *Computers & Geosciences, v. 28*, no. 9, p. 1061-8.
Modeling the AMS to strain relationship is complex due to: different carriers and their magnetic properties, their initial orientation distribution, the manner in which the deformation influences the reorientation of magnetic carriers, the character and duration of deformation. These parameters are taken into account in a new package of Matlab functions which can be freely combined by the user to cover all basic types of homogeneous deformation (simple shear, pure shear, plane strain, coaxial deformation, transpression). A procedure is presented to treat the example of inhomogeneous deformation.

Environmental Magnetism and Paleoclimate Proxies

Moreno, E., Thouveny, N., Delanghe, D., McCave, I. N., and Shackleton, N. J., 2002, **Climatic and oceanographic changes in the Northeast Atlantic reflected by magnetic properties of sediments deposited on the Portuguese Margin during the last 340 ka**: *Earth and Planetary Science Letters, v. 202*, no. 2, p. 465-80.
In cores MD95-2040 and MD95-2042, thin discrete layers containing coarse grains of titanomagnetite (TM) are associated with Heinrich events 1-6. Concentrations of fine-grained TM and hematite/goethite vary in phase opposition, with Milankovitch periods at 100 and 41 ka, and a tight correlation with the D-O cycles in Greenland ice records. The nature (TM) and size range of the finest ferrimagnetic fraction suggest control by deep currents carrying a colloidal/clayey fraction from remote sources (Iceland, Faeroes, MAR). Variation of hematite/goethite contents is linked with transport by rivers and winds from the neighbouring continent.

Ortega, B., Caballero, C., Lozano, S., Israde, I., and Vilaclara, G., 2002, **52000 years of environmental history in Zacapu basin, Michoacan, Mexico: the magnetic record**: *Earth and Planetary Science Letters, v. 202*, no. 3, p. 663-75.
Curie temperature measurements, low-temperature susceptibility and low-temperature remanence indicate oxidized titanomagnetites with variable Ti content. Low S300 ratios reflect high-coercivity iron oxide phases, probably goethite rather than hematite, formed in relatively wet, organic conditions. Comparison of magnetic and TOC results suggests relatively humid conditions before 35 kyr BP, and a later trend towards drier conditions. A probable hiatus is recorded before 25 kyr, and relatively dry conditions persisted throughout the Late Glacial Maximum and Mid Holocene, to 4.8 kyr.

Extraterrestrial Magnetism

Weiss, B. P., Vali, H., Baudenbacher, F. J., Kirschvink, J. L., Stewart, S. T., and Shuster, D. L., 2002, **Records of an ancient Martian magnetic field in ALH84001**: *Earth and Planetary Science Letters, v. 201*, no. 3, p. 449-63.
4 Ga carbonates containing magnetite and pyrrhotite carry a stable NRM, and $^{40}Ar/^{39}Ar$ thermochronology suggests that the NRM originated at 3.9-4.1 Ga on Mars. The strong intensity suggests that within 450-650 Myr of its formation, Mars had a global magnetic field with a surface intensity within an order of magnitude of that of the present-day Earth, sufficient for magnetotaxis by the bacteria whose magnetofossils have been reported in ALH84001 and possibly for the production of the strong crustal anomalies. Chromite in ALH84001 may retain even older records of Martian magnetic fields, possibly extending back to near the time of planetary formation.

Instruments and Techniques

Gilder, S. A., LeGoff, M., Peyronneau, J., and Chervin, J. C., 2002, **Novel high pressure magnetic measurements with application to magnetite**: *Geophysical Research Letters, v. 29*, no. 10, p. 30-4.
Using a novel diamond anvil cell system we find that reversible hysteresis parameters for magnetite vary <15% below 0.6 to 1.0 GPa, while at higher pressures significant increases occur in H_c and M_{rs}/M_s. The net effect of pressure is to displace magnetite toward a truer single domain state. Our data, together with the fact that magnetite Curie temperature increases with pressure, suggest that magnetite can account for geomagnetic anomalies related to some subduction zones and potentially to meteorite impact sites on Earth, as well as magnetic signatures observed on some planetary bodies like Mars.

Hill, M. J., Gratton, M. N., and Shaw, J., 2002, **A comparison of thermal and microwave palaeomagnetic techniques using lava containing laboratory induced remanence**: *Geophysical Journal International, v. 151*, no. 1, p. 157-63.
Three samples containing a laboratory induced TRM were subjected to microwave palaeointensity experiments (using the Liverpool 8.2 GHz system). Conventional Thellier palaeointensity experiments were carried out on the same three lava samples, this time containing a known microwave induced TRM (TMRM). Both techniques produced the correct intensity value,

demonstrating the equivalence of TRM and TMRM. In a second set of experiments, six samples were given a TRM and a perpendicular pTRM. Sister samples were then demagnetised using thermal and microwave methods. Analysis of the orthogonal vector plots (OVPs) revealed little difference in separating the two components for five out of the six samples.

Magnetic Field Records and Paleointensity Methods

Bin, G., Zhu, R., and Florindo, F., 2002, **A short, reverse polarity interval within the Jaramillo subchron: evidence from the Jingbian section, northern Chinese Loess Plateau**: *Journal of Geophysical Research, v. 107*, no. B6, p. EMP2-1-12.

Bohnel, H., and Molina-Garza, R., 2002, **Secular variation in Mexico during the last 40,000 years**: *Physics of the Earth and Planetary Interiors, v. 133*, no. 1, p. 99-109.

Brown, L., 2002, **Paleosecular variation from Easter Island revisited: modern demagnetization of a 1970s data set**: *Physics of the Earth and Planetary Interiors, v. 133*, no. 1, p. 73-81.

Channell, J. E. T., Mazaud, A., Sullivan, P., Turner, S., and Raymo, M. E., 2002, **Geomagnetic excursions and paleointensities in the Matuyama Chron at Ocean Drilling Program Sites 983 and 984 (Iceland Basin)**: *Journal of Geophysical Research, v. 107*, no. B6, p. EMP1-1-14.

Frank, U., Nowaczyk, N. R., Negendank, J., and Melles, M., 2002, **A paleomagnetic record from Lake Lama, northern Central Siberia**: *Physics of the Earth and Planetary Interiors, v. 133*, no. 1, p. 3-20.

Frank, U., Schwab, M. J., and Negendank, J. F. W., 2002, **A lacustrine record of paleomagnetic secular variations from Birkat Ram, Golan Heights (Israel) for the last 4400 years**: *Physics of the Earth and Planetary Interiors, v. 133*, no. 1, p. 21-34.

Gogorza, C. S. G., Sinito, A. M., Lirio, J. M., Nunez, H., Chaparro, M., and Vilas, J. F., 2002, **Paleosecular variations 0-19,000 years recorded by sediments from Escondido Lake (Argentina)**: *Physics of the Earth and Planetary Interiors, v. 133*, no. 1, p. 35-55.

Goguitchaichvili, A., Alva-Valdivia, L. M., Urrutia, J., Morales, J., and Lopes, O. F., 2002, **On the reliability of Mesozoic dipole low: new absolute paleointensity results from Parana Flood Basalts (Brazil)**: *Geophysical Research Letters, v. 29*, no. 13, p. 33-1.

Hatakeyama, T., and Kono, M., 2002, **Geomagnetic field model for the last 5 My: time-averaged field and secular variation**: *Physics of the Earth and Planetary Interiors, v. 133*, no. 1, p. 181-215.

Heller, R., Merrill, R. T., and McFadden, P. L., 2002, **The variation of intensity of Earth's magnetic field with time**: *Physics of the Earth and Planetary Interiors, v. 131*, no. 3, p. 237-49.

Herrero-Bervera, E., and Valet, J. P., 2002, **Paleomagnetic secular variation of the Honolulu volcanic series (33-700 ka), O'ahu (Hawaii)**: *Physics of the Earth and Planetary Interiors, v. 133*, no. 1, p. 83-97.

Horng, C.-S., Lee, M.-Y., Palike, H., Wei, K.-Y., Liang, W.-T., Iizuka, Y., and Torii, M., 2002, **Astronomically calibrated ages for geomagnetic reversals within the Matuyama chron**: *Earth, Planets and Space, v. 54*, no. 6, p. 679-90.

Kruiver, P. P., Langereis, C. G., Dekkers, M. J., Davies, G. R., and Smeets, R. J., 2002, **The implications of non-suppressed geomagnetic secular variation during the Permo-Carboniferous Reversed Superchron**: *Physics of the Earth and Planetary Interiors, v. 131*, no. 3, p. 225-35.

Oda, H., Nakamura, K., Ikehara, K., Nakano, T., Nishimura, M., and Khlystov, O., 2002, **Paleomagnetic record from Academician Ridge, Lake Baikal: a reversal excursion at the base of marine oxygen isotope stage 6**: *Earth and Planetary Science Letters, v. 202*, no. 1, p. 117-32.

Plenier, G., Camps, P., Henry, B., and Nicolaysen, K., 2002, **Palaeomagnetic study of Oligocene (24-30 Ma) lava flows from the Kerguelen Archipelago (southern Indian Ocean): directional analysis and magnetostratigraphy**: *Physics of the Earth and Planetary Interiors, v. 133*, no. 1, p. 127-46.

Quidelleur, X., Carlut, J., Gillot, P. Y., and Soler, V., 2002, **Evolution of the geomagnetic field prior to the Matuyama-Brunhes transition: radiometric dating of a 820 ka excursion at La Palma**: *Geophysical Journal International, v. 151*, no. 2, p. F6-10.

Takai, A., Shibuya, H., Yoshihara, A., and Hamano, Y., 2002, **Paleointensity measurements of pyroclastic flow deposits co-born with widespread tephras in Kyushu Island, Japan**: *Physics of the Earth and Planetary Interiors, v. 133*, no. 1, p. 159-79.

Tanaka, H., and Kono, M., 2002, **Paleointensities from a Cretaceous basalt platform in Inner Mongolia, northeastern China**: *Physics of the Earth and Planetary Interiors, v. 133*, no. 1, p. 147-57.

Yamazaki, T., 2002, **Long-term secular variation in geomagnetic field inclination during Brunhes Chron recorded in sediment cores from Ontong-Java Plateau**: *Physics of the Earth and Planetary Interiors, v. 133*, no. 1, p. 57-72.

Magnetic Microscopy and Spectroscopy

Korecki, P., and Korecki, J., 2001, **Site selectivity in gamma-ray holography**: *Hyperfine Interactions, v. 136*, p. 3-4.
The possibility of imaging the local environments of nuclei with different hyperfine interaction parameters using complex gamma-ray holography is investigated. The discussion is based on calculations performed for magnetite Fe_3O_4, in which Fe ions occupy two nonequivalent positions in the unit cell characterized by different sets of hyperfine interaction parameters.

Ziese, M., Hohne, R., Esquinazi, P., and Busch, P., 2002, **Micromagnetic studies of magnetite films using μ -Hall sensor arrays**: *Physical Review B, v. 66*, no. 13, p. 134408-1-8.
The local-field distribution on magnetite films fabricated on MgO and $MgAl_2O_4$ substrates was measured with a μ-Hall sensor array. The stray-field hysteresis loops observed here mainly consist of a hysteretic contribution and superimposed field spikes near the coercive field. From an analysis of these Hall data, magnetization and magnetic force microscopy measurements as well as micromagnetic simulations it is concluded that the local field arises from (i) magnetic domain tilt, (ii) out-of-plane domains due to a broad easy axis distribution, and (iii) stray fields emanating from domain walls.

Magnetization Processes

Gapeev, A. K., and Gribov, S. K., 2002, **Partial self-reversal of the thermoremanent magnetization created by titanomagnetites subjected to multiphase oxidation**: *Izvestiya, Physics of the Solid Earth, v. 38*, no. 9, p. 713-22.
Partial self-reversal of TRM occurs in titanomagnetite (TM) subjected to multiphase oxidation. The self-reversal effect is shown to arise in x = 0.6 TM at two different temperatures: a high-temperature self-reversal in the spinel phase as a result of the interaction between regions differing in their properties due to the compositional heterogeneity, and a low-temperature oxidation caused by the interaction between the spinel and rhombohedral phases. Experiments on the creation of CRM due to multiphase oxidation of TM were carried out. In some cases, the CRM was found to experience complete self-reversal.

Tan, X., Kodama, K. P., and Fang, D., 2002, **Laboratory depositional and compaction-caused inclination errors carried by haematite and their implications in identifying inclination error of natural remanence in red beds**: *Geophysical Journal International, v. 151*, no. 2, p. 475-86.
Red bed samples were disaggregated to make silt-dominated and clay-sized sediment slurries. During compaction clay-sized sediments experienced 17-19° inclination shallowing at 58° magnetic field inclination, while coarser sediments showed little laboratory compaction-caused inclination error. Acquisition of IRM, coercivity spectra and unblocking temperature spectra reveal that the magnetic carrier for the fine-grained sample is dominated by pigmentary haematite. The coarse-grained sediments showed a range of depositional inclination error, 0° -30°, carried by larger high unblocking temperature/ coercivity particles.

Mineral & Rock Magnetism

Hu, S., Stephenson, A., and Appe, E., 2002, **A study of gyroremanent magnetisation (GRM) and rotational remanent magnetisation (RRM) carried by greigite from lake sediments**: *Geophysical Journal International, v. 151*,

no. 2, p. 469-74.
The GRM produced during static AF demagnetisation became close to its maximum at a peak AF of 150 mT. The GRM of a crushed sample was much reduced because of the destruction of the sample's anisotropy, although as expected, both RRM and effective gyrofield (Bg) were similar before and after crushing, demonstrating that RRM and Bg are independent of anisotropy. Measurement of the anisotropy of two samples from different depths showed that the deeper sample, which acquired the higher GRM, also had the higher anisotropy presumably as a result of greater sediment compaction. Study of anisotropy of GRM may help to elucidate the preferred alignment of greigite within the sample, which is difficult to ascertain by other means.

Ishikawa, N., and Frost, G. M., 2002, **Magnetic properties of sediments from Ocean Drilling Program sites 1109, 1115, and 1118 (Leg 180), Woodlark Basin (Papua New Guinea)**: *Earth, Planets and Space, v. 54*, no. 9, p. 883-97.
Miocene-Pleistocene synrift sediments, located on the hanging wall margin north of the Moresby fault, show variations in magnetite and maghemite related to sedimentation process in the basin. An increase in the ferrimagnetic mineral concentrations occurred between 3.4 Ma and 3.2 Ma at the three sites. The onset age of the change decreases with distance from the subsidence center of the basin, which implies a northward onlapping of sediments with high ferrimagnetic mineral concentration. Sediments with finer-grained ferrimagnetic minerals were deposited between 2.3 and 2.0 Ma at sites 1118 and 1109 and later, 2.8 Ma at Site 1115 during a period of a low sedimentation rate.

Walz, F., Brabers, J. H. V. J., and Brabers, V. A. M., 2002, **The Verwey transition in magnetite as studied by means of definite impurity doping**: *Zeitschrift fur Metallkunde, v. 93*, no. 10, p. 1095-102.
The effect of low-dose cation doping ($0.005 < x < 0.08$) of magnetite single crystals, $Fe_{3-x}M_xO_4$ (M = Ni, Mg, Co, Al, Ti, Ga), has been studied by means of the magnetic after-effect (MAE) spectroscopy with respect to (i) the Verwey transition, (ii) the low-temperature ($4\ K < T < 125\ K \approx T_V$) charge transport mechanisms and (iii) the zero-crossing of the crystal anisotropy. Variations of the MAE spectra clearly indicate the low-temperature tunnelling ($4\ K < T < 35\ K$) to be far more affected by smallest impurity doping than variable long-range hopping ($50\ K < T < 125\ K$)- this outstanding sensibility of the tunnelling processes against impurities or any other defects is also true when compared with the corresponding T_V shifting. All samples undergo a doping-induced temperature splitting, ΔT_{VC}, between the Verwey transition (spontaneous jump of the susceptibility at T_V) and the zero-crossing of the crystal anisotropy (giving rise to a delayed susceptibility maximum)- in contrast to perfectly stoichiometric Fe_3O_4 single crystals where both effects are coincident. This range of temperature-splitting ΔT_{VC}, found to be extremely large in the case of Co^{2+} doping, is characterized by destabilized magnetic domain structures due to locally disordered anisotropy distribution in the lattice.

Modeling and Theory

Tamura, I., and Mizushima, T., 2002, **Explanation for magnetic properties of interacting iron oxide nanocrystals**: *Journal of Magnetism and Magnetic Materials, v. 250*, no. 1, p. 241-8.
To explain the results of magnetization measurements and Mössbauer measurements on interacting iron oxide nanocrystals which have been produced by leaving iron nanoparticles in air of 1 atm for 10 years, we propose the following model. Several tens of the oxide nanocrystals randomly cohere to form a cluster. As a result, we assume that each nanocrystal within a cluster has random unidirectional magnetic anisotropy, and that the clusters are weakly interacting each other at random. The super-spin-glass model is used for analyzing the random interaction among the clusters.

Synthesis and Properties of Magnetic Materials

Cote, L. J., Teja, A. S., Wilkinson, A. P., and Zhang, Z. J., 2002, **Continuous hydrothermal synthesis and crystallization of magnetic oxide nanoparticles**: *Journal of Materials Research, v. 17*, no. 9, p. 2410-16.
The continuous hydrothermal synthesis of nanoparticles of two metal oxides (α-Fe_2O_3 and Co_3O_4) is described. Two variations of the technique were investigated, involving the precipitation reaction between a metal salt solution and a hydroxide solution at ambient conditions and at elevated temperatures. Elevated temperatures resulted in more uniform particles of α-Fe_2O_3 and Co_3O_4, although the actual sizes of the particles were apparently unaffected by the temperature. This behavior was attributed to the species present in solution and the solubilities of the cation(s), both of which were calculated via a thermodynamic model for the systems under study.

Del Bianco, L., Fiorani, D., Testa, A. M., Bonetti, E., Savini, L., and Signoretti, S., 2002, **Magnetothermal behavior of a nanoscale Fe/Fe oxide granular system**: *Physical Review B, v. 66*, no. 17, p. 174418-1-11.
The low-temperature magnetic properties of samples obtained by cold-compacting core-shell Fe/Fe oxide nanoparticles have been investigated, as well as their dependence on the structure, composition, and mean particle size. The results support the existence of a low-temperature (below T_1~20 K) frozen, disordered magnetic state, characterized by a strong exchange coupling between the structurally disordered, spin-glass-like oxide matrix and the Fe nanocrystallites. Above T_1, a quasi-static, ferromagnetic component, given by the Fe particles, coexists with a relaxing component, represented by regions of exchange-interacting spins of the oxide matrix.

Khollam, Y. B., Dhage, S. R., Potdar, H. S., Deshpande, S. B., Bakare, P. P., Kulkarni, S. D., and Date, S. K., 2002, **Microwave hydrothermal preparation of submicron-sized spherical magnetite (Fe_3O_4) powders**: *Materials Letters, v. 56*, no. 4, p. 571-7.
Submicron-sized (0.15-0.2 μm) spherical agglomerates of magnetite (Fe_3O_4) powders have been prepared successfully by microwave hydrothermal (MH) reaction of ferrous sulphate and sodium hydroxide in the temperature range of 90-200° C. X-ray powder diffraction patterns of all these powders indicated that the product is single-phase magnetite with cubic spinel structure having lattice parameter, $a_0 = 8.392$ Å. The kinetics of MH synthesis is one order faster than the reported conventional hydrothermal (CH) synthesis.

Ngo, A. T., and Pileni, M. P., 2002, **Cigar-shaped ferrite nanocrystals: orientation of the easy magnetic axes**: *Journal of Applied Physics, v. 92*, no. 8, p. 4649-52.
Mesoscopic structures made of cigar-shaped γ-Fe_2O_3 nanocrystals with an average length of 325 nm and aspect ratio of 7 are described. The structures were prepared starting from an aqueous solution to which a magnetic field parallel to the substrate could be applied during the evaporation process. If a magnetic field was applied, the nanocrystals rotated their long axis along the magnetic field direction to form ribbons, whereas without a field the nanocrystals remained deposited on the substrate with a random orientation. The orientation of the nanocrystals is responsible for the anisotropy of the ribbons as evidenced by the hysteresis loops.

Roy, R., Peelamedu, R., Hurtt, L., Jiping, C., and Agrawal, D., 2002, **Definitive experimental evidence for microwave effects: radically new effects of separated E and H fields, such as decrystallization of oxides in seconds**: *Materials Research Innovations, v. 6*, no. 3, p. 128-40.
The present study has been conducted, for the first time, in a single mode TE103 cavity at 2.45 GHz, at positions of the E field and H field maxima. The most extraordinary effects and the sharpest differences (noted to date) between reactions at the E and H nodes have been found in ferroic oxides. Phases such as Fe_3O_4 are rendered non-crystalline to XRD in a few seconds in the H field, although they show no bulk evidence for melting. The microstructures are unique, showing smooth glasslike regions with regular waves parallel to each other. In the E field node the identical pellet components react completely and form large euhedral crystals of a single phase. The phenomenon of decrystallization or formation of nano-glasses was confirmed for all the 3d ferrite phases.

Tago, T., Hatsuta, T., Miyajima, K., Kishida, M., Tashiro, S., and Wakabayashi, K., 2002, **Novel synthesis of silica-coated ferrite nanoparticles prepared using water-in-oil microemulsion**: *Journal of the American Ceramic Society, v. 85*, no. 9, p. 2188-94.
Ferrite nanoparticles (magnetite (Fe_3O_4) and cobalt-ferrite ($Co_xFe_{3-x}O_4$)) coated with silica (SiO_2) were prepared using water-in-oil microemulsion of a polyoxyethylene(15)cetylether/cyclohexene system. Observation via transmission electron microscopy revealed that the ferrite nanoparticles were located nearly at the center of spherical SiO_2 particles. The sizes of Fe_3O_4 and $Co_xFe_{3-x}O_4$ nanoparticles were in the range of 8-12 nm and 10-14 nm, respectively, and the thickness of the SiO_2 layer was 14.0 nm.

...Calibration
continued from p. 1

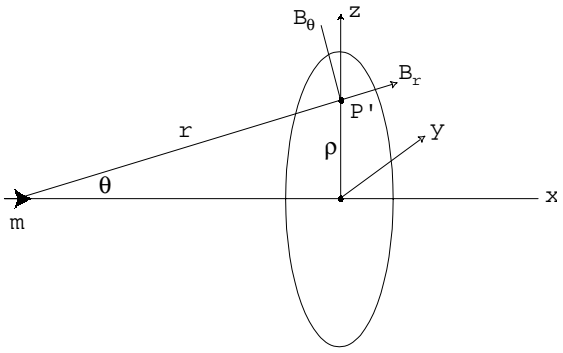

Fig 1. dipole-coil geometry for part 1 of calibration by calculation

reliable standard. However, in principle, calculation of the relationship is also possible for many instruments, either analytically or numerically, if the geometry is defined with sufficient precision. This calibration-by-calculation approach was used by LakeShore Cryotronics for their series 7000 AC susceptometers.

It is interesting to work through the calculations. (If you disagree, you may skip the next few paragraphs.) First let's look at flux linkage between a planar circular coil of radius A and a point magnetic dipole of moment m, located on the coil axis at a perpendicular distance x, and oriented coaxially (see fig 1). At an arbitrary point P' in the plane of the coil, the field due to the dipole has components

$B_r = \mu_0 m \cos\theta / (2 \pi r^3)$ and

$B_\theta = \mu_0 m \sin\theta / (4 \pi r^3)$

where r and θ refer to the polar coordinate system of the dipole. The component normal to the plane of the coil is

$B_n = B_r \cos\theta - B_\theta \sin\theta$.

Integration over the planar area A bounded by the coil gives the flux

$\Phi = \frac{1}{2} \mu_0 m A^2 (A^2 + x^2)^{-3/2}$.

The flux is thus proportional to the dipole moment and to the coil-dipole geometry.

As shown by Faraday and by Henry, a change in flux produces a voltage, and many/most magnetometers and susceptometers operate by measuring the voltage generated by time-varying flux. This can be accomplished by changing the geometry (e.g., translating the dipole, as in a VSM) and/or by changing the dipole moment (as in an ac susceptometer). The voltage v is:

$$v = \oint \vec{E} \cdot \vec{ds} = \int_{area} (\nabla \times \vec{E}) \cdot \vec{dA}$$

$$= -\int_{area} (d\vec{B}/dt) \cdot \vec{dA} = -d\Phi/dt$$

In other words, the voltage is the line integral of the tangential component of electric field around the coil, which by a theorem of Stokes is equal to the surface integral, over the coil area, of the normal component of the curl of E. The latter integrand in turn is equated by Faraday's law to the normal component of $d\mathbf{B}/dt$, whose surface integral is the the flux. For a coil with multiple turns, the voltage is multiplied by N.

For the LakeShore, the sensing coil is not a planar coil but a solenoid, with a length somewhat greater than its diameter (see *IRM Quarterly v*. 12, n. 1 for a diagram). The total flux linkage between a solenoidal coil, of diameter D and length L, and an axial dipole moment $\boldsymbol{m}$ centered in the coil, is obtained by integrating the planar coil flux over the length of the solenoid:

$$\Phi = \int_{x=-L/2}^{L/2} \frac{\mu_0 m A^2 n}{2(A^2 + x^2)^{3/2}} dx$$

$$= \frac{\mu_0 m L n}{(A^2 + L^2)^{1/2}} = \gamma \cdot m$$

where n is the number of windings per unit length. As in the planar coil case, the flux is proportional to m, the constant of proportionality being determined by the coil-dipole geometry.

In an applied ac field H, m varies sinusoidally with time, and therefore so does the resulting voltage over the sensing coil. The measured ac voltage v is related to susceptibility by:

$v = \gamma\, dm/dt = \gamma\, kV\, dH/dt$

with an rms value of

$v_{rms} = \gamma\, k\, V f H_{rms}$

f and V being AC frequency and sample volume, respectively. Thus,

$k = \alpha\, v_{rms} / (V f H_{rms})$

where $\alpha = 1/\gamma$.

The factor α, which depends only on instrument/sample geometry, is the primary calibration constant for the LakeShore susceptometer. For the instrument at the *IRM*, α has a value of 1.757 A m²/(V s). The LakeShore documentation reports that the calculated values are experimentally validated by measurements using NIST SRM 766 MnF_2, but the calculated value is still considered the primary calibration.

This approach of calibration-by-calculation has various advantages and disadvantages, compared to calibration by material standards. One advantage is that it enables evaluation of, and correction for, the effects of variable sample size and shape (see *IRM Quarterly v*. 11 n. 4), although the calculations become much more difficult for non-pointlike samples. Based on calculations by Goldfarb and Minervini [1984], the LakeShore documentation provides an explicit quantification of the variation in calibration as a function of length for cylindrical specimens. For a typical 15-mm gelcap specimen, the calibration coefficient α is about 8% larger than it is for a pointlike specimen. The calibration-by-calculation approach also eliminates some of the problems and uncertainties associated with maintaining standard materials, such as contamination by minute amounts of strongly magnetic materials.

A drawback of the calculation approach is that some simplifying assumptions must be made, for example that eddy currents in surrounding conductive materials may be neglected. These may not always be valid, and the calibration is only as good as the assumptions. Another major advantage of material standards is the fact that they are not limited to a specific instrument, but can be used for absolute or relative calibration of various instruments (provided they are sufficiently close to the size and shape of the samples measured on the instrument). Material standards are also extremely useful for detecting and diagnosing subtle instrument problems or malfunctions. Finally, for some instruments the geometry is too variable for the calculation approach to be pratical. For example, it is possible to calibrate a VSM by calculation [see, e.g., Kelso et al., 2002], but we commonly widen the pole gap to accomodate large samples, or narrow it to maximize sensitivity and/or applied field strength, and it is a quick and simple matter to calibrate each time by running a standard sample of known saturation moment.

Calibration using test coils

The use of test coils lies somewhere between the approaches discussed above, i.e., use of material standards and calibration by calculation. A specimen-sized coil carrying a DC current has a steady dipole moment that can be calculated precisely, given the coil geometry and current. This provides an accurate alternative means of calibrating DC magnetometers [Noltimeier, 1964]. There are practical drawbacks that limit the applicability and/or effectiveness of this approach in some cases, however. For a spinner magnetometer, for example, it is necessary to have a sliding-contact arrangement, and for RF SQUID instruments inductive RF coupling is a problem. For these reasons, we have not relied very heavily on test coils for calibration at *IRM*.

How accurate?

For many kinds of magnetic measurements, it is surprisingly difficult to attain accuracies better than a few percent using any of the methods described above. Numerous small sources of error that can

Calibration
continued on p. 8...

be neglected in routine measurements become significant when high accuracy is required. Some of the more significant are sample size/shape effects, temperature, centering, and sample holder/contamination, and we briefly discuss each of these below.

Temperature. Even in a controlled-climate laboratory, "room temperature" covers a range of a few degrees C, enough to change paramagnetic susceptibility by at least 1%. Moreover local temperatures may vary even more significantly. For example, the VSMs at IRM use chilled (~12° C) water to cool their electromagnets. The pole pieces equilibrate to a similar temperature, and samples in the pole gap, if left in place for sufficient time, equilibrate at about 14°. Variability in room temperature is most significant for paramagnetic susceptibility measurements and for magnetization measurements on materials such as goethite and Ti-rich titanomagnetites, for which spontaneous magnetization is a strong function of T in the range around 290-300 K.

Sample holder signal and sample contamination. For weakly-magnetic specimens, the limiting factor in obtaining valid data is often not instrument noise but background signals. For example, the nominal sensitivity of the MPMS instruments is 10^{-11} A m^2. In practice it is nearly impossible to evaluate the actual sensitivity, because the cleanest "blank" (empty sample holder) we have been able to produce has a remanent moment of 10^{-9} A m^2, 100 times higher than the noise limit. Further, even perfectly clean materials can generate significant signals related to edges and discontinuities in an applied field. The Quantum Design documentation describes their methodology for measuring calibration standards. Each standard cylinder was inserted into a fused quartz tube (as pictured on page 1), whose inner diameter (3 mm) slightly exceeded that of the cylinder . Matching 3-mm-diameter solid quartz rods were then inserted from each end to hold the palladium cylinder rigidly in place. "Blank" measurements made with the same arrangement, containing an air gap in place of the standard cylinder, yielded a signal 2.3% as strong as that of the palladium, due to stray fields from the ends of the diamagnetic quartz rods!

Centering. Instruments that use gradiometer sensing coil arrays (including the MPMS and VSMs) require accurate centering to produce accurate measurements. In some cases (e.g., MPMS), each moment determination involves systematic displacement of the sample through the center position, with numerous measurements along the scan length. The moment is then calculated by fitting a dipole curve to the data scan. This reduces moment errors due to mispositioning to well under 1%. However with other instruments (e.g. VSMs) or other measurement types (e.g., AC susceptibility measurements on MPMS) systematic scans are not routinely made after initial centering, and because of the sharp gradients in instrument response, errors of at least 5% are very common if samples are not carefully centered.

Sample size/shape effects. If measured samples differ in size and/or shape from the standards used for instrument calibration, errors of more than 10% may easily result (*IRM Quarterly v*. 11 n. 4). Again because of sharp spatial variations in instrument response, gradiometer instruments are most vulnerable to errors of this sort. (These geometric effects are also closely related to the convolution problem in whole-core magnetometry, which we will avoid here, restricting our attention to discrete samples).

IRM intralab calibration

Over the years we have routinely cross-calibrated the instruments at the *IRM* using a variety of standards, each of which is suitable for one or more instruments (fig. 2). In addition to the manufacturer-supplied standards, we use:
paramagnetic rare-earth oxides (Dy_2O_3 and Gd_2O_3) for AC susceptibility calibration. They are nonconductive, and therefore more suitable than Pd for AC measurements. They also have mass suceptibilities 20-50 times higher than that of palladium, and powders can easily be packed into containers of different size and shape.
hard ferromagnets (Nd-Fe-B and aluminum-substituted titanomagnetite (ATM)) for zero-field DC moment calibration. These have remanent moments that are utterly stable, immune to the action of ambient fields, to variation in room temperature, and to the ravages of time. The ATM was synthesized and given its thermoremanence by Özden Özdemir, and experience has proven it to be superior to all other magnetites, hematites, recording tape, and other materials we have tried over the past twenty years. The thermoremanent moment of 2.29 μAm^2 fits comfortably into the dynamic range of both the 2G SQUID and the Schoenstedt spinner, and it can also be measured with the MPMS and MicroMag instruments. Our neodymium-iron-boron magnets have only been in use for a year or two, but they also appear to be quite stable and reliable.
soft ferromagnets (Ni spheres, mu-metal) for saturation moment calibration. Before the *IRM*, before the MicroMags and MPMSs, the primary rock-magnetic instrument in our lab was a PAR VSM (which is still heavily used for room-temperature hysteresis measurements on large samples). The main calibration standard for this instrument is a nickel (99.999%) sphere, with a whopping 2.298 mAm^2 saturation moment, near the upper limit for the newer PMC VSMs.

Ideally, of course, these calibrations should be perfectly consistent: the same standard measured on any instrument should produce exactly the same moment or susceptibility. How well do they actually match in practice? The answer is that it depends to a certain extent on what you compare and how you measure, but in general, with sufficient attention to temperature, centering, and size/shape effects, everything agrees within 2-3%. There are slight but fairly sytematic differences between groups of instruments. In the middle group, the LakeShore 7130, the two MPMS instruments, and the PAR VSM are usually within 1% of each other for susceptibility measurements on Dy_2O_3 or Gd_2O_3; our Kappabridge often gives values 2-3% lower than the other instruments, at the same temperature. For saturation magnetization and DC susceptibility, the MicroMags give average values 1-2% higher than the MPMS, even for measurements of the Ni-foil and Pd standards supplied by the respective manufacturers.

An important consequence is that one must exercise critical judgement when combining data from different instruments. For example, we often wish to quantify ferrimagnetic and paramagnetic contributions to low-field susceptibility ($k=k_f + k_p$). Taking the linear high-field slope of a hysteresis loop as the best estimate of k_p, and subtracting this from low-field AC susceptibility ($k_f + k_p$), we obtain an estimate of k_f. Clearly the individual measurement and calibration errors, though small in proportion to the original measurements, may be large in relation to their difference. When the low-field and high-field measurements are made on different instruments, (e.g., Kappabridge and VSM), it is not uncommon to find the physically-impossible result $k_p > k_f + k_p$ (i.e., $k_f < 0$) for paramagnetically-dominated specimens. Measurement of both properties on a single instrument (e.g., MPMS) eliminates errors due to calibration and to spatial variations in sensitivity.

MAG-NET interlab calibration

An extremely worthwhile interlaboratory calibration study last year was led by Leonardo Sagnotti (INGV, Roma) and Pierre Rochette (CEREGE, Aix-en-Provence), and

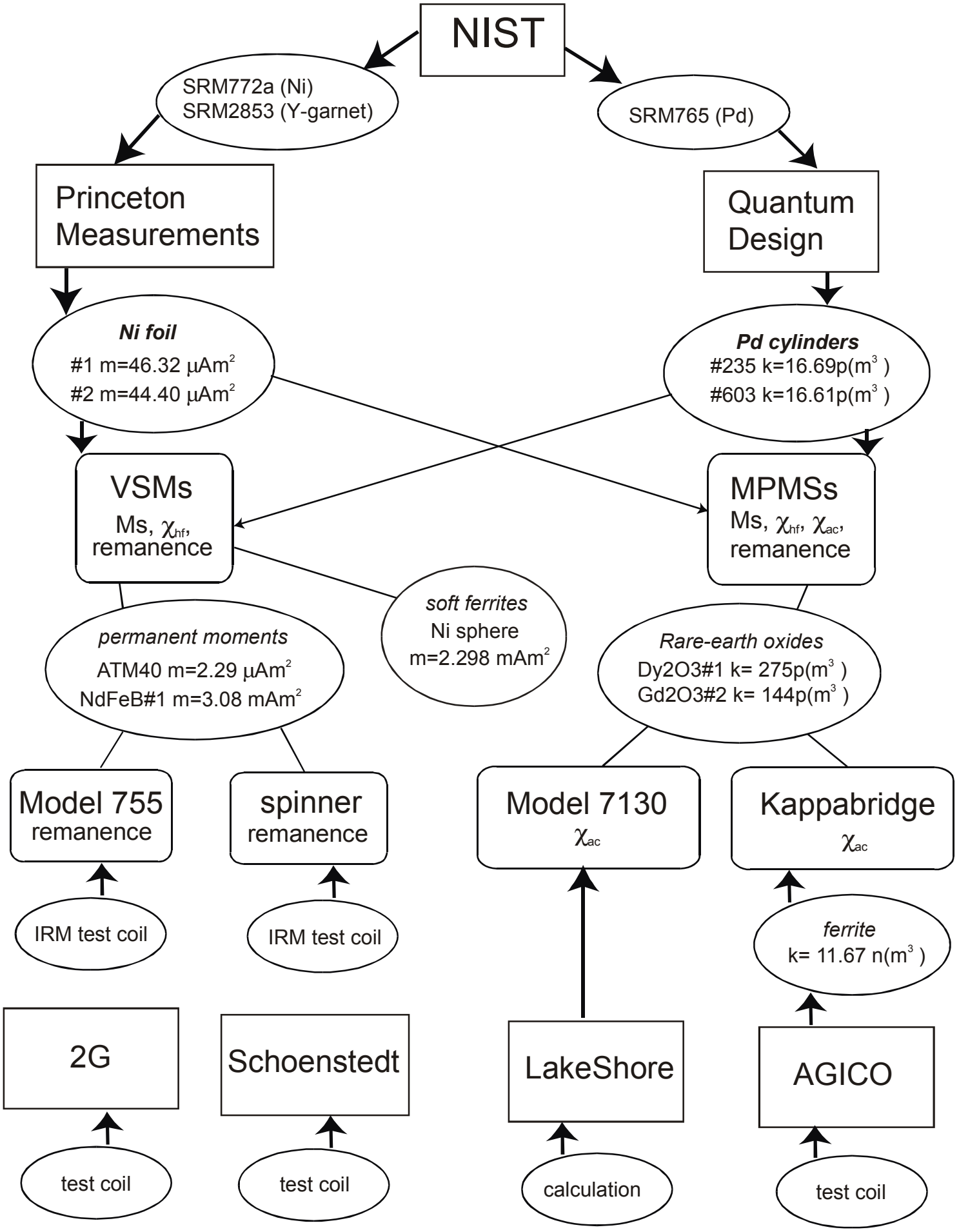

Fig. 2. Primary calibration paths (bold arrows) for the instruments at IRM. Finer lines show additional inter-instrument calibration routes. All moment and susceptibility calibrations are traceable to NIST standards.

involved labs of the MAG-NET consortium (Lancaster, Leoben, Liverpool, Madrid, Marseille, München, Roma, Southampton, Utrecht, and Zürich), as well as Bremen and *IRM*. The study involved three types of measurement: low-field AC susceptibility (Gd_2O_3 and magnetite-bearing Pozzolana cement), remanent moment (cement with an anhysteretic remanence imprinted before distribution), and anhysteretic susceptibility (the same cement remagnetized in each lab with a new ARM).

The results are not too dissimilar to our intralab cross-calibrations. Kappabridge measurements from 10 labs had a standard deviation of 1.3%. Bartington MS2B results showed a bit more scatter, with a standard deviation of 4.1%, and a mean about 3% lower than that of the Kappa measurements. Sagnotti et al [2003] note that the mean susceptibility measured by the 10 Kappabridges is ~5% lower than the "book" value for Gd_2O_3.

Measurements of the original ARM were made on various magnetometers, including 2G SQUIDs (DC and RF), and Molspin and AGICO JR5 spinners. Consistency was rather good, with a standard deviation of 3.4%. Surprisingly, however, the variability in the new ARMs produced in the different labs was *much* greater, with a standard deviation of 20.5%.

This large variability clearly is not due to incorrect magnetometer calibration, since the original ARM measurements produced much more consistent results. It is the process of imparting new ARMs that is the major cause of the inconsistency, and decay rate of the alternating field is the prime suspect. This underscores the need for more complete "system calibration," involving not only measurements of moment and susceptibility, but also processes of magnetization, if data from different labs are to be compared in a meaningful way.

Calibration and data exchange

A challenge facing the development of the rock and paleomagnetic database is to meld data from many different labs into a standardized form. Unit conversions, data formats and computer platforms are a few of the conversions that can be automated. Heating and cooling rates, geometry, and AF decay rates are all factors that need to be accounted for if we are to have a self-consistent and truly useful international, inter-laboratory database.

Accurate moment calibrations are of fundamental importance for quantitative applications involving data from different labs. This is no simple task, as we have seen, given the different means of calibration and different calibration standards available. Although it would be nice to assume that every instrument and all the data produced from it are calibrated and exact, in practice this assumption can get us into trouble if we try to carry it too far. Here at the *IRM*, our rule of thumb is to expect differences of up to 2% for different instruments when each is properly calibrated with a standard of the same geometry as the specimens being analyzed. Errors of 20% or more are easy to obtain when the geometry of calibration standards and specimens differ (e.g., non-point source samples such as paleomagnetic cylinders, sediment packed in cubes, cores and split cores, gel-caps of material, etc.). Geometry problems aside, a 2% error can be a problem for research involving pure materials.

Of course we realize that for many purposes, accuracy of moment or susceptibility determinations is not critical. Given the orders-of-magnitude variation in magnetic properties of natural materials, a calibration uncertainty of a few percent is, for many applications, completely negligible. Further, many significant properties (coercivities, M_R/M_S ratios, and Curie temperatures, for example) can be accurately determined from normalized or uncalibrated moment data, provided other parts of the experimental system (temperature, applied field, etc.) are properly calibrated. Likewise, valid and significant conclusions can be made through qualitative comparison of miscalibrated but self-consistent data sets from a single instrument or laboratory. Nevertheless, calibration and accuracy are vital concerns for a public shared database, where calibration mismatches may lead to incorrect interpretations and conclusions.

Without more precise inter-lab calibration, data cataloged in the database will not be fully useful for quantitative applications. In addition to fundamental moment calibrations, it is necessary to account for other major potential sources of error, including variations in sample geometry and in magnetization procedures. This is not to say that these difficulties will prevent a database from being a useful research tool. Rather, building the database will help to establish standards for data acquisition and processing, which will help provide solid footing for the future of rock and paleo-magnetic research and will help push for the quantification of environmental magnetic research.

In the near future, we plan to develop a set of standard materials at *IRM* for interlaboratory exchange and cross-calibration efforts. We will tie these to our existing traceable standards, and to our recently-purchased NIST SRM 2853 yttrium-iron garnet standard.

References

Goldfarb, R. B., Lelental, M., and Thompson, C. A., 1992, Alternating-field susceptometry and magnetic susceptibility of superconductors, *in* Hein, R. A., Francavilla, T. L., and Liebenberg, D. H., eds., *Magnetic Susceptibility of Superconductors and Other Spin Systems*: New York, Plenum.

Kelso, P. R., Tikoff, B., Jackson, M., and Sun, W., 2002, A new method for the separation of paramagnetic and ferromagnetic susceptibility anisotropy using low field and high field methods: *Geophysical Journal International, v. 151*, no. 2, p. 345-59.

Noltimeier, H. C., 1964, Calibration of a spinner magnetometer with a wire loop: *Journal of Scientific Instruments, v. 41*, p. 55.

Özdemir, Ö., 1981, Laboratory synthesis of aluminium-substituted titanomaghemites and their characteristic properties: *Journal of Geophysics, v. 49*, p. 93–100.

Özdemir, Ö., and O'Reilly, W., 1982, An experimental study of thermoremanent magnetization acquired by synthetic monodomain titanomagnetite substituted by aluminium: *Geophysical Journal of the Royal Astronomical Society, v. 70*, p. 141–154.

Sagnotti, L. et 24 al., 2003, Interlaboratory calibration of low-field (k) and anhysteretic (k_a) susceptibility measurements, *Physics of the Earth and Planetary Interiors*, in press.

For More Information

http://www.metallurgy.nist.gov/magnet/srm.htm

http://ts.nist.gov/ts/htdocs/230/232/232.htm

http://www.qdusa.com/resources/pdf/mpmsappnotes/1041-001.pdf

Sturgeon, William

b. May 22, 1783, Whittington, North Lancashire
d. Dec 4, 1850, Prestwick, Manchester

Apprenticed to a shoemaker at the age of 10, he later ran off to join the military. Intrigued about the nature of lightning, he borrowed books and taught himself Latin, mathematics and physics. He became popular for his shock-inducing kites, and after leaving the military at age 37 began a lecturing and research career. Following the work of Ampere and Arago, Sturgeon developed the first practical electromagnet, using 16 turns of wire wrapped around a horseshoe-shaped piece of iron (coated with varnish for insulation) which could lift 4 kg, about 20 times its own weight. For this he received he the silver medal of the Royal Society of Arts in 1825. In addition Sturgeon invented the commutator (1832) used in electric motors, an electromagnetic rotary engine (1832) and a dynamo (1823).

New Visiting Fellows

The new Visiting Fellows (spring 2003) have been selected, based on evaluations from the RAC. The Fellows and their projects are:

Charly Aubourg (*Université Cergy Pontoise*) Normal polarity behavior of Tertiary CRM in remagnetized carbonates from SE Alps.

Pavel Doubrovine (*University of Rochester*) Self-reversal of remanent magnetization carried by titanomaghemite in submarine basalts

Belén Oliva Urcia (*Universidad de Zaragoza*) Discontinuous deformation as a mechanism of remagnetization of limestones in the Internal Sierras (Southern Pyrenees, Spain).

Xixi Zhao (*University of California Santa Cruz*) Detecting oxidation state of magnetite-bearing basalts using low-temperature magnetic data and Mössbauer spectra

Tragelephas strepsiceros, the greater kudu

RAC Rotation

The *IRM*'s Review and Advisory Committee (RAC) has undergone a scheduled rotation of membership. **Ken Kodama** (*Lehigh University*) completed his six-year tour of duty, which including chairing the RAC for the last two years. **Pierre Rochette** (*CEREGE*) has joined the RAC, and **Rob Coe** (*UC-Santa Cruz*) has become the new chair.

The RAC is an autonomous panel of external experts, and as its name indicates, the RAC fills two important roles in *IRM* operations. First, it provides long-term strategic guidance. *IRM* is a shared resource for the entire geomag/paleomag/rockmag/environmental-magnetic research community; the RAC represents the interests of that community, and helps to ensure that *IRM* policies and operations are designed with the broad interests of the community in mind. Second, the RAC is responsible for evaluating Visiting Fellowship proposals, again with the goal of making the best possible use of the *IRM* facilities.

In addition to Rob and Pierre, the current RAC members are: **Jim Channell** (*University of Florida*), **Lisa Tauxe** (*Scripps*), **Ron Merrill** (*University of Washington*), **Roy Roshko** (*University of Manitoba*), and **Cor Langereis** (*Utrecht University*).

We extend hearty thanks to Ken for his leadership and commitment over the last six years.

Kudos: IRM Students Win Best Paper Awards

Both **France Lagroix** and **Brian Carter-Stiglitz** have been selected for Outstanding Student Paper Awards, for their invited presentations at the 2002 Fall Meeting of the American Geophysical Union in San Francisco. France's talk, in the session on "The Use of Magnetic Properties as a Petrologic Tool," was entitled "*The Magnetic Fingerprint of Alaskan Loess from Their Modern and Buried Soils to Their Petrostratigraphic Markers*." Brian's presentation, "*Numerical Modeling of the Low-temperature Magnetism of SSD Magnetite*", was in the session on "Numerical Modeling in Geomagnetism/ Paleomagnetism."

Nota Bene: New Application Deadlines

For many of us, December is a horribly busy time, with AGU meetings, NSF proposal deadlines, final exams, and holiday preparations all requiring time and attention. For that reason, we have decided to move the deadline for *IRM* Visiting Fellowships out of December, in order to make it easier for more people to apply. The new application deadlines are:

➨ **April 30** (for visits from July 1 through December 31)

➨ **October 30** (for visits from January 1 through June 30)

Visiting Fellowships provide access to the entire set of IRM instruments (as needed), for periods up to ten days. Visiting Fellowships are also eligible for reimbursement of travel expenses (up to a maximum of $750; lodging and meal costs excluded).

IRM Visiting Fellowship Proposal Preparation Guidelines

1.Proposal Length: Do not exceed a total of three pages for the text, figures, and references in your project description. Be concise. Excessive proposal length is a good way to antagonize the members of our Review and Advisory Committee (RAC).

2.Subject Areas: Topics for research are open to any field of study involving fine particle magnetism, but preference will be given to projects relating magnetism to geological or environmental studies, or to fundamental physical studies that are of potential relevance to the geosciences. In the latter case, you should give a brief indication of the relevance.

3.Justification: Briefly explain the overall importance of your project, and why it is important for you to carry out detailed studies at the IRM. In general, projects that require only widely-available equipment (such as paleomagnetic or low-field susceptibility instruments) will be given lower priority than those that require a variety of more specialized rock-magnetic instruments (e.g., low-temperature, high-field susceptometers, domain imaging, Mössbauer spectroscopy).

4.Work Plans: Outline the experiments to be carried out or data to be acquired during your visit.

For application forms and further information, please see our web site (http://www.geo.umn.edu/orgs/irm/visiting/index.htm)

The *Institute for Rock Magnetism* is dedicated to providing state-of-the-art facilities and technical expertise free of charge to any interested researcher who applies and is accepted as a Visiting Fellow. Short proposals are accepted semi-annually in spring and fall for work to be done in a 10-day period during the following half year. Shorter, less formal visits are arranged on an individual basis through the Facilities Manager.

The *IRM* staff consists of **Subir Banerjee**, Professor/Director; **Bruce Moskowitz**, Professor/Associate Director; **Jim Marvin**, Senior Scientist; **Mike Jackson**, Senior Scientist and Facility Manager, and **Peat Sølheid**, Scientist.

Funding for the *IRM* is provided by the **National Science Foundation**, the **W. M. Keck Foundation**, and the **University of Minnesota**.

The *IRM Quarterly* is published four times a year by the staff of the *IRM*. If you or someone you know would like to be on our mailing list, if you have something you would like to contribute (*e.g.*, titles plus abstracts of papers in press), or if you have any suggestions to improve the newsletter, please notify the editor:

Mike Jackson
Institute for Rock Magnetism
University of Minnesota
291 Shepherd Laboratories
100 Union Street S. E.
Minneapolis, MN 55455-0128
phone: (612) 624-5274
fax: (612) 625-7502
e-mail: irm@umn.edu
www.geo.umn.edu/orgs/irm/irm.html

IRM

UNIVERSITY OF MINNESOTA

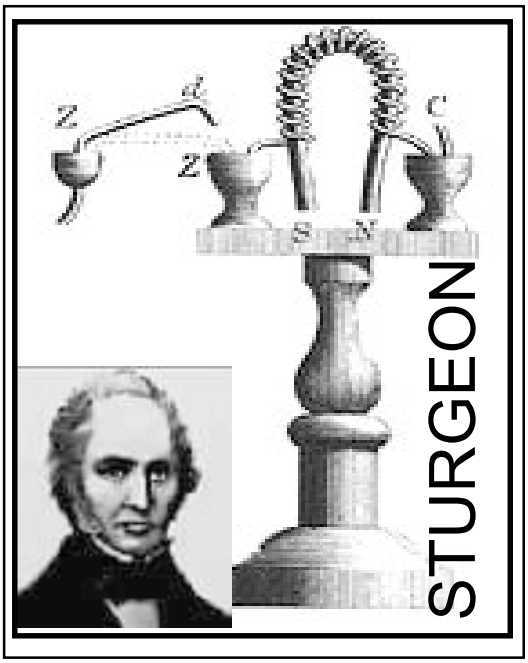

Collector's Series #27

http://chem.ch.huji.ac.il/~eugeniik/history/sturgeon.html

Note new Visiting Fellowship application deadlines! Details inside...

The IRM Quarterly

University of Minnesota
291 Shepherd Laboratories
100 Union Street S. E.
Minneapolis, MN 55455-0128
phone: (612) 624-5274
fax: (612) 625-7502
e-mail: irm@umn.edu
www.geo.umn.edu/orgs/irm/irm.html

Nonprofit Org.
U.S Postage
PAID
Mpls., MN
Permit No. 155